Bujalowski, W., & Lohman, T. M. (1986) *Biochemistry 25*, 7799–7802.
Bujalowski, W., & Lohman, T. M. (1987) *J. Mol. Biol. 195*, 897–907.
Bujalowski, W., Overman, L. B., & Lohman, T. M. (1988) *J. Biol. Chem. 263*, 4629–4640.
Carmichael, G. G., & McMaster, G. K. (1980) *Methods Enzymol. 65*, 380–391.
Chase, J. W., & Williams, K. R. (1986) *Annu. Rev. Biochem. 55*, 103–136.
Chrysogelos, S., & Griffith, J. (1982) *Proc. Natl. Acad. Sci. U.S.A. 79*, 5803–5807.
Epstein, I. R. (1978) *Biophys. Chem. 8*, 327–339.
Gear, C. W. (1971) *Commun. ACM 14*, 185–189.
Greipel, J., Maass, G., & Mayer, F. (1987) *Biophys. Chem. 26*, 149–161.
Greipel, J., Urbanke, C., & Maass, G. (1989) in *Topics in Nucleic Acids Research* (Neidle, T. S., Ed.) pp 61–86, Macmillan, London.
Krauss, G., Sindermann, H., Schomburg, U., & Maass, G. (1981) *Biochemistry 20*, 5346–5352.
Lohman, T. M. (1983) *Biopolymers 22*, 1697–1713.
Lohman, T. M. (1986) *CRC Crit. Rev. Biochem. 19*, 191–245.
Lohman, T. M., & Overman, L. B. (1985) *J. Biol. Chem. 260*, 3594–3603.
Lohman, T. M., Green, J. M., & Beyer, R. S. (1986a) *Biochemistry 25*, 21–25.
Lohman, T. M., Overman, L. B., & Datta, S. (1986b) *J. Mol. Biol. 187*, 603–615.
McGhee, J. D., & VonHippel, P. H. (1974) *J. Mol. Biol. 86*, 469–489.
Ollis, D. B. P., Abdel-meguid, S. S., Murthy, K., Chase, J. W., & Steitz, T. A. (1983) *J. Mol. Biol. 170*, 797–800.
Powell, M. D. (1965) *Comput. J. 7*, 303–307.
Reckmann, B., Grosse, F., Urbanke, C., Frank, R., & Bloecker, H. (1985) *Eur. J. Biochem. 152*, 633–644.
Römer, R., Schomburg, U., Krauss, G., & Maass, G. (1984) *Biochemistry 23*, 6132–6137.
Ruyechan, W. T., & Wetmur, J. G. (1976) *Biochemistry 15*, 5057–5062.
Sancar, A., Williams, K. R., Chase, J. W., & Rupp, W. D. (1981) *Proc. Natl. Acad. Sci. U.S.A. 78*, 4274–4278.
Schneider, R. J., & Wetmur, J. G. (1982) *Biochemistry 21*, 608–615.
Schomburg, U. (1985) Thesis, Universität Hannover.
Schwarz, G., & Watanabe, F. (1983) *J. Mol. Biol. 163*, 467–484.
Walmsley, A. R., & Bagshaw, C. R. (1989) *Anal. Biochem. 176*, 313–318.
Williams, K. R., Spicer, E. K., LoPresti, M. B., Guggenheimer, R. A., & Chase, J. W. (1983) *J. Biol. Chem. 258*, 3346–3355.
Yamamoto, K. R., Alberts, B. M., Benzinger, R., Lawhorn, L., & Treiba, G. (1970) *Virology 40*, 734–744.

Characterization of the Multiple Catalytic Activities of Tartrate Dehydrogenase†

Peter A. Tipton* and Jack Peisach
Department of Molecular Pharmacology, Albert Einstein College of Medicine, Bronx, New York 10461
Received July 27, 1989; Revised Manuscript Received October 19, 1989

ABSTRACT: Tartrate dehydrogenase (TDH) has been purified to apparent homogeneity from *Pseudomonas putida* and has been demonstrated to catalyze three different NAD^+-dependent reactions. TDH catalyzes the oxidation of (+)-tartrate to form oxaloglycolate and the oxidative decarboxylation of D-malate to form pyruvate and CO_2. D-Glycerate and CO_2 are formed from *meso*-tartrate in a reaction that is formally a decarboxylation with no net oxidation or reduction. The steady-state kinetics of the first two reactions have been investigated and found to follow primarily ordered mechanisms. The pH dependence of V and V/K was determined and indicates that catalysis requires that a base on the enzyme with a pK of 6.7 be unprotonated. TDH activity requires a divalent and a monovalent cation. Kinetic data suggest that the cations function in substrate binding and facilitation of the decarboxylation of β-ketoacid intermediates.

The study of the stereospecificity of microbial metabolism of tartaric acid has a long history; Duclaux (1920) noted that Pasteur observed that *Penicillium* was able to grow on a racemic solution of ammonium tartrate. As growth progressed, the solution acquired optical activity. After the cessation of growth, the solution contained only levo-rotatory tartrate, demonstrating that the microorganisms were able to utilize only one isomer of tartrate.

More recently, the pathways for utilization of (+)-tartrate, (−)-tartrate, and *meso*-tartrate in *Pseudomonas* have been elucidated, and many of the enzymes involved have been isolated (Clarke & Ornston, 1975). Kohn et al. (1968) reported the isolation and characterization of a tartrate dehydrogenase from a strain of *Pseudomonas putida* which required Mn^{2+} and K^+ for activity and catalyzed the oxidation of both (+)-tartrate and *meso*-tartrate to oxaloglycolate. Because these requirements for inorganic cofactors were relatively novel for a dehydrogenase, we set out to determine their functions in the reported catalytic reactions. We now wish to report that when *P. putida* is grown on a mixture of (+)-tartrate and *meso*-tartrate as the sole carbon sources, an enzyme is produced which catalyzes the conversion of (+)-tartrate to oxaloglycolate, *meso*-tartrate to D-glycerate and CO_2, and D-malate to pyruvate and CO_2. In other words, for these three similar substrates, the same enzyme catalyzes

† Supported by NIH Grant GM 40168. P.A.T. is supported by NIH Postdoctoral Fellowship GM 12081.

0006-2960/90/0429-1749$02.50/0

oxidation without decarboxylation [(+)-tartrate to oxaloglycolate], decarboxylation without net oxidation (*meso*-tartrate to D-glycerate), and oxidative decarboxylation (D-malate to pyruvate). In this paper, we describe the purification of this enzyme, define the kinetic mechanism of the (+)-tartrate and D-malate oxidative reactions, and describe the divalent and monovalent metal ion specificities and the pH dependence of some of the kinetic parameters.

Materials and Methods

Alcohol dehydrogenase, lactate dehydrogenase, malate dehydrogenase, and glyoxalate reductase were purchased from Sigma, as were all common biochemicals.

Cell Growth. *Pseudomonas putida* ATCC 17642, the strain from which Kohn et al. (1968) reported the isolation of tartrate dehydrogenase (TDH),[1] was obtained from the American Type Culture Collection and was grown on media containing 1.1 g of K_2HPO_4, 0.48 g of KH_2PO_4, 1 g of NH_4NO_3, 0.25 g of $MgSO_4 \cdot 7H_2O$, 2 g of (+)-tartrate, and 0.2 g of *meso*-tartrate, per liter. The inorganic salts were sterilized by autoclaving, and the tartrates were sterilized by passage through a 0.22-μm filter. Distilled water that had been further purified by passage through a Millipore Milli Q system of deionizing filters was used in all the media since it was discovered that the distilled water originally used contained sufficient Ca^{2+} to precipitate most of the tartrate. Cultures were maintained at 4 °C on agar slants consisting of the same media. Cells were grown at room temperature in a 45-L carboy that was vigorously aerated. After 15 h, the cells were harvested by centrifugation at 5000*g*. The cell paste was washed once with 20 mM potassium phosphate, pH 7.2, frozen in liquid nitrogen, and stored at −90 °C.

Assays. The rate of (+)-tartrate oxidation was determined by monitoring the formation of NADH at 340 nm (ϵ = 6220 M^{-1} cm^{-1}) in reaction mixtures containing 10 mM K_2·(+)-tartrate, 1.5 mM NAD^+, 0.4 mM $Mn(OAc)_2$, and 1 mM DTT in 100 mM HEPES, pH 8.0. D-Malate oxidation was monitored in the same way, except that 0.5 mM D-malate replaced (+)-tartrate in the reaction mixture. In order to determine the products of the D-malate assay, some reactions were carried out in the presence of malate dehydrogenase and lactate dehydrogenase. All assays were carried out in 1-cm path-length quartz cuvettes at 25 °C in a total volume of 1 mL, and activity of the enzyme was defined by the (+)-tartrate oxidation reaction, one unit being that amount of enzyme which catalyzes the formation of 1 μmol of oxaloglycolate per minute, under the conditions of the assay described above. Protein concentration was determined by the method of Bradford (1976), using the Bio-Rad protein assay reagent and bovine serum albumin as standard. Catalytic oxidation of D-malate and (+)-tartrate was detected after native gel electrophoresis by staining with a solution of 0.24 mM nitro blue tetrazolium, 0.4 mM $Mn(OAc)_2$, 1.5 mM NAD^+, and 1.0 mM D-malate or 10 mM (+)-tartrate, in 100 mM K^+-HEPES, pH 8.0. Turnover of *meso*-tartrate was detected under the same conditions, except that 1.0 mM *meso*-tartrate was added instead of D-malate or (+)-tartrate, and 0.8 unit of glyoxalate reductase was added to couple formation of D-glycerate to NADH production.

Purification of Tartrate Dehydrogenase. Forty grams of frozen cell paste was suspended in 40 mL of 20 mM potassium phosphate buffer, pH 7.2, containing 1 mM DTT. Immediately prior to cell disruption, the protease inhibitors phenylmethanesulfonyl fluoride, dissolved in acetone, and N^a-*p*-tosyllysine chloromethyl ketone were each added to final concentrations of 0.5 mM. The suspended cells were disrupted by sonication with a Branson Model 450 sonifier with a 0.5-in. tip operating at 75% maximum power on a 50% duty cycle. The cell suspension was sonicated 3 times for 2 min with cooling between each sonification and then centrifuged for 30 min at 10 °C at 25000*g*. The supernatant was set aside, and the pellet was resuspended in 40 mL of 20 mM potassium phosphate, pH 7.2, containing 1 mM DTT. Protease inhibitors were added again to final concentrations of 0.5 mM, and the sonifications and centrifugation were repeated. All subsequent steps, except for the heat treatment (see below), were performed at 4 °C.

The supernatants from the two centrifugations were combined, and 24 mL of an 8.3 mg/mL solution of protamine sulfate was added dropwise, and the solution was stirred for an additional 20 min. The precipitated nucleic acids were removed by centrifugation at 20000*g* for 15 min.

The supernatant (approximately 180 mL) contained in a 600-mL stainless-steel beaker was placed in a water bath at 58 °C. The solution was stirred for 10 min and then quickly cooled on ice. After the solution was cooled, the precipitated protein was removed by centrifugation at 20000*g* for 15 min.

A Pharmacia FPLC apparatus was used to chromatograph the supernatant from the heat step. The protein was loaded onto a 5 × 28 cm column of Pharmacia Fast Flow Q anion-exchange resin, equilibrated in 15 mM triethanolamine, pH 7.8, containing 1 mM DTT. TDH was eluted from the column using a 3-L gradient from 0 to 1 M NaCl in the above buffer. The enzyme eluted in approximately 0.4 M NaCl.

The active fractions from the anion-exchange chromatography were pooled and dialyzed against 6 L of the triethanolamine and DTT buffer described above. The desalted protein was then loaded onto a 2.5 × 6.5 cm column of poly(ethylenimine)–cellulose, equilibrated in the same buffer. The column was washed with 50 mL of the equilibration buffer, followed by 50 mL of buffer containing 0.45 M NaCl. TDH was eluted with 200 mL of buffer containing 0.9 M NaCl. Active fractions were pooled and dialyzed against the triethanolamine/DTT buffer.

The dialyzed protein was concentrated via ultrafiltration with an Amicon PM30 membrane and chromatographed using a Pharmacia FPLC apparatus. The protein was loaded 20 mg at a time onto a 1.6 × 51 cm column of Superose 6B, equilibrated in the triethanolamine/DTT buffer containing 100 mM NaCl. The column was eluted at 1.0 mL/min. TDH eluted in a single well-resolved peak after 70 min; fractions containing the enzyme were pooled and concentrated by ultrafiltration.

^{1}H NMR Analysis of the Tartrate Dehydrogenase Reaction Products. ^{1}H NMR spectra of the species produced by the action of TDH on *meso*-tartrate and D-malate were obtained in order to identify the reaction products. The enzyme used for preparing the NMR samples was equilibrated with 200 mM ammonium formate, pH 8.0, containing 1 mM DTT and 50 mM KCl, by passage over a column of Sephadex G-25. The D-malate reaction mixture contained 0.04 unit of TDH, 5 mM D-malate, 0.2 mM NAD^+, 0.4 mM $Mn(OAc)_2$, 9 mM acetaldehyde, and 1500 units of alcohol dehydrogenase. The *meso*-tartrate reaction contained 0.2 unit of TDH, 5 mM *meso*-tartrate, 0.35 mM NAD^+, and 0.4 mM $Mn(OAc)_2$. Both reactions were carried out in the ammonium formate buffer described above, in a total volume of 1 mL. The re-

[1] Abbreviations: DTT, dithiothreitol; HEPES, *N*-(2-hydroxyethyl)-piperazine-*N*′-2-ethanesulfonic acid; MES, 2-(*N*-morpholino)ethanesulfonic acid; Tris, tris(hydroxymethyl)aminomethane; TEA, triethanolamine; SDS–PAGE, sodium dodecyl sulfate–polyacrylamide gel electrophoresis; TDH, tartrate dehydrogenase.

Table I: Purification of Tartrate Dehydrogenase

step	activity[a] (units)	protein (mg)	sp act. (units/mg)	yield (%)	x-fold purification	ratio of D-malate act. to (+)-tartrate act.
cell-free extract	45.2	3168	0.014	100		45
protamine sulfate	48	3275	0.015	106	1.1	49
heat	62.9	874	0.072	139	5.1	31
Fast Flow Q	55	177.6	0.310	122	22.1	29
poly(ethyleneimine)–cellulose	27.2	66.2	0.411	60	29.4	34
Superose 6B	28.6	49.1	0.582	63	41.6	33

[a] Activity is defined by the oxidation of (+)-tartrate as described under Materials and Methods.

action mixtures were incubated at room temperature for 18 h, the protein was removed by ultrafiltration using Amicon Centricon 30 filters, and the filtrates were diluted to 10 mL with H_2O. Each sample was stirred for 15 min with 1 g of Chelex-100 to remove the Mn^{2+}. The resin was filtered off, and the filtrates were reduced to dryness by rotary evaporation. Each sample was dissolved in 0.75 mL of D_2O and placed in a 5-mm NMR tube. 3-(Trimethylsilyl)propionic-*2,2,3,3-d*$_4$ acid was added as a chemical shift standard. ^1H NMR spectra were obtained by using a Varian VXR spectrometer operating at 500 MHz.

Steady-State Kinetics. The (+)-tartrate and D-malate oxidation reactions were examined by initial velocity kinetics studies. Reactions were followed at 25 °C by monitoring NADH production with a Gilford 260 spectrophotometer equipped with thermospacers and attached to a circulating water bath. NAD^+ and D-malate solutions were calibrated by enzymatic end-point assays with glucose-6-phosphate dehydrogenase and TDH, respectively. Oxalacetate solutions were calibrated by end-point assay with malate dehydrogenase. Dilute $Mn(OAc)_2$ solutions were prepared fresh daily from a 0.20 M stock solution. All reactions were carried out in 100 mM HEPES, pH 8.0, except when the pH dependence of the kinetic parameters was being determined, when 100 mM HEPES or MES were used in their appropriate ranges. Because TDH is activated by potassium, all buffers were adjusted to the desired pH with KOH. The pH studies were carried out in the presence of 50 mM KCl (>10 times the K_m of K^+) to minimize the effect of differences in K^+ concentration in buffers at different values of pH. Initial velocity data were fitted to the appropriate equations using BASIC translations of the FORTRAN programs of Cleland (1979). Data were fitted to eq 1 when one substrate was varied in the presence of

$$v = \frac{VA}{K + A} \quad (1)$$

saturating levels of the other substrates. When the (+)-tartrate or D-malate concentration was varied in the presence of different levels of NAD^+, data were fitted to eq 2. Initial velocity

$$v = \frac{VAB}{K_aB + K_bA + AB + K_{ia}K_b} \quad (2)$$

data obtained by varying the level of free D-malate or free (+)-tartrate at different levels of free Mn^{2+} or Mg^{2+} were fitted to eq 3. For these experiments, the levels of free metal

$$v = \frac{VAB}{K_{ia}K_b + K_bA + AB} \quad (3)$$

and free ligand were calculated on the basis of stability constants of M^{2+}-tartrate and M^{2+}-malate given in Martell and Smith (1979).

Inhibition data were fitted to eq 4–6, which describe competitive, uncompetitive, and noncompetitive inhibition, respectively.

$$v = \frac{VA}{K(1 + I/K_i) + A} \quad (4)$$

$$v = \frac{VA}{K + A(1 + I/K_i)} \quad (5)$$

$$v = \frac{VA}{K(1 + I/K_{is}) + A(1 + I/K_{ii})} \quad (6)$$

Data obtained for the variation of V and V/K with pH were fitted to eq 7, which describes the reduction in rate which occurs upon protonation of a single base, where C is the pH-independent value of the kinetic parameter.

$$\log V \text{ (or } V/K) = \log\left(\frac{C}{1 + H/K_a}\right) \quad (7)$$

Metal Ion Specificity. The ability of various divalent metal ions to support the TDH-catalyzed oxidation of (+)-tartrate was investigated. The buffer and all substrate stock solutions were treated with Chelex-100 before use. Reactions were carried out in the presence of 10 mM (+)-tartrate, 1.5 mM NAD^+, 1 mM DTT, and 0.4 or 4 mM divalent metal, in 100 mM K^+-HEPES, pH 8.0. Full kinetic patterns for the oxidation of (+)-tartrate and D-malate in the presence of Mn^{2+} and Mg^{2+} were carried out, as described in Table II.

The monovalent cation specificity of TDH in the (+)-tartrate and D-malate reactions was also investigated. These assays were carried out in 100 mM Tris, pH 8.0, and stock solutions of all the substrates were prepared from the free acids. The reactions contained 20 mM (+)-tartrate or 0.5 mM D-malate, 1.2 mM NAD^+, 0.5 mM $Mn(OAc)_2$, and 1 mM DTT; monovalent cation concentrations were varied from 2.0 to 50 mM.

Results

Purification of Tartrate Dehydrogenase. The purification scheme used for obtaining TDH is summarized in Table I. The heat stability of the enzyme allows the use of a heat treatment step which greatly simplifies the purification. All other operations are carried out at 4 °C, however, to minimize protease activity. Addition of protease inhibitors also enhances the yield of TDH. The presence of a thiol reagent appears to be critical for maintaining enzyme activity; enzyme that is inactive due to the absence of DTT does regain activity upon its addition.

TDH obtained by these means appears homogeneous as determined by SDS–PAGE. Purified enzyme is stable at 4 °C in 10% glycerol for several months. Several criteria were used to determine that the observed catalytic activities arise from a single protein. All three activities comigrate under nondenaturing conditions on polyacrylamide gels. The

Table II: Steady-State Kinetic Parameters for Oxidation of (+)-Tartrate and D-Malate by Tartrate Dehydrogenase

variable substrate	fixed variable substrate	fixed substrate	K_m (mM)	K_i (mM)	pattern
			(+)-Tartrate Oxidation		
(+)-tartrate	NAD^+	0.4 mM Mn^{2+}	1.08 ± 0.12 [(+)-tartrate] 0.12 ± 0.01 (NAD^+)		intersecting
(+)-tartrate	Mn^{2+}	1.2 mM NAD^+	1.72 ± 0.08 [(+)-tartrate]	0.058 ± 0.004 (Mn^{2+})	rapid equilibrium ordered
NAD^+	Mn^{2+}	2 mM (+)-tartrate	0.10 ± 0.01 (NAD^+)	0.045 ± 0.005 (Mn^{2+})	rapid equilibrium ordered
(+)-tartrate	Mg^{2+}	1.5 mM NAD^+	1.38 ± 0.06 [(+)-tartrate]	2.05 ± 0.16 (Mg^{2+})	rapid equilibrium ordered
			D-Malate Oxidation		
D-malate	NAD^+	0.4 mM Mn^{2+}	0.058 ± 0.005 (D-malate) 0.050 ± 0.005 (NAD^+)		intersecting
D-malate	Mn^{2+}	0.6 mM NAD^+	0.056 ± 0.005 (D-malate)	0.076 ± 0.009 (Mn^{2+})	rapid equilibrium ordered
D-malate	Mg^{2+}	1.5 mM NAD^+	0.057 ± 0.019 (D-malate)	1.64 ± 0.64 (Mg^{2+})	rapid equilibrium ordered

(+)-tartrate- and D-malate-dependent activities exhibit identical temperature dependences. Thermal denaturation studies were carried out by maintaining aliquots of TDH at elevated temperatures for 10 min and then assaying for oxidation of (+)-tartrate and D-malate. TDH is fully active after 10 min at 65 °C, retains half of its catalytic activity after 10 min at 72 °C, and is inactivated after 10 min at 78 °C.

Steady-state kinetic studies further demonstrated that TDH alone is responsible for turnover of (+)-tartrate, *meso*-tartrate, and D-malate. Since *meso*-tartrate turnover does not result in net production of NADH, it can be tested as an inhibitor versus D-malate. Similarly, since (+)-tartrate oxidation is much slower than D-malate oxidation (see below), it can also be tested as an inhibitor versus D-malate. Observation of competitive inhibition patterns in both experiments indicates that binding of *meso*-tartrate and D-malate is mutually exclusive, as is binding of (+)-tartrate and D-malate. (These experiments were carried out in the presence of a large excess of Mn^{2+} to preclude apparent inhibition by metal chelation.) These data support the supposition that all three substrates bind to the same site on a single protein. The K_i for *meso*-tartrate is 15.8 ± 0.9 μM; the K_i for (+)-tartrate is 1.61 ± 0.13 mM, which is comparable to its K_m (see below).

Finally, the ratio of D-malate dehydrogenase activity to (+)-tartrate dehydrogenase activity remains constant through the last steps of the purification. The apparent decrease in this ratio through the first steps of the purification is attributable to inhibition of (+)-tartrate dehydrogenase activity in the crude extract. Although inhibition of the (+)-tartrate dehydrogenase activity without a corresponding inhibition of the D-malate activity seems to contradict the assertion that the two activities arise from a single enzyme, it is likely that D-malate, for which tartrate dehydrogenase has a 30-fold greater affinity than for (+)-tartrate, is simply able to outcompete the inhibitor, whereas (+)-tartrate cannot. Also, when individual fractions from the gel filtration column are assayed for (+)-tartrate and D-malate dehydrogenase activities, the ratio of the two activities remain constant across the peak of enzyme activity. Therefore, we believe that the (+)-tartrate and D-malate dehydrogenase activities, as well as the *meso*-tartrate decarboxylase activity, are intrinsic to a single protein. Ebbighausen and Giffhorn (1984) have earlier demonstrated that TDH isolated from *Rhodopseudomonas sphaeroides* grown on *meso*-tartrate as the sole carbon source catalyzes the same three reactions that we report here.

SDS–PAGE of purified TDH indicates that it has a subunit molecular weight of 38 000. Chromatography on Pharmacia Superose 6B resin indicates that the native protein has a molecular weight of 77 000, suggesting that it is a dimer of identical subunits. It is difficult to know what is the relationship between the tartrate dehydrogenase that we isolated and the one described by Kohn et al. (1968). Although our protein is isolated from the same strain that was used by Kohn et al. in their investigations, we were unable to grow the bacteria under the conditions reported by Kohn et al., i.e., using *meso*-tartrate as the sole carbon source.[2] We obtained two cultures from the American Type Culture Collection; neither would grow on *meso*-tartrate. The bacteria did grow on (+)-tartrate, however, and it was found that (+)-tartrate dehydrogenase activity was elevated in crude extracts obtained from cells grown on a 10:1 mixture of (+)-tartrate and *meso*-tartrate. The enzyme that we isolate from these cells has a number of features in common with the TDH described by Kohn et al. Both enzymes exhibit similar monovalent and divalent cation specificities, and the subunit molecular weights appear the same. However, the protein we isolated appears to be a dimer, whereas the enzyme of Kohn et al. (1968) is a tetramer.

Table III: Inhibition Constants for the Tartrate Dehydrogenase Reactions

inhibitor	varied substrate	inhibition pattern[a]	K_{ii} (mM)	K_{is} (mM)
		(+)-Tartrate Oxidation		
NADH	NAD^+	C		0.030 ± 0.002
NADH	(+)-tartrate	NC	0.44 ± 0.09	0.061 ± 0.010
OAA	NAD^+	UC	0.082 ± 0.004	
OAA	(+)-tartrate	C		0.021 ± 0.002
		D-Malate Oxidation		
pyruvate	D-malate	NC	3.98 ± 0.57	1.30 ± 0.18
NADH	NAD^+	C		0.032 ± 0.002

[a] C is competitive inhibition, NC is noncompetitive inhibition, and UC is uncompetitive inhibition.

Steady-State Kinetics. In the presence of Mn^{2+}, V_{max} for the oxidation of (+)-tartaric acid is 0.71 ± 0.02 μmol min^{-1} (mg of TDH)$^{-1}$. Michaelis constants and dissociation constants derived from initial velocity studies are presented in Table II. When the (+)-tartrate concentration is varied at fixed levels of NAD^+, the reciprocal plot consists of a family of lines intersecting to the left of the ordinate, indicating that the two substrates bind to the enzyme in a steady-state sequential manner. When either the free (+)-tartrate or NAD^+ concentration is varied at fixed levels of free Mn^{2+}, a pattern intersecting on the ordinate is obtained. These patterns indicate that Mn^{2+} binding is in rapid equilibrium and occurs

[2] Because our studies with the purified TDH demonstrate that the enzyme is capable of turning over *meso*-tartrate, the inability of the bacteria to grow on *meso*-tartrate suggests that they are unable to absorb it from the media. Shilo and Stanier (1957) have noted that *Pseudomonas* appear to have a separate permease for each stereoisomer of tartrate. We have observed that increasing the level of *meso*-tartrate in the media, while keeping (+)-tartrate constant, severely inhibits the growth of the bacteria, suggesting that *meso*-tartrate can also inhibit the uptake of (+)-tartrate (P. Tipton, unpublished observations).

Scheme I

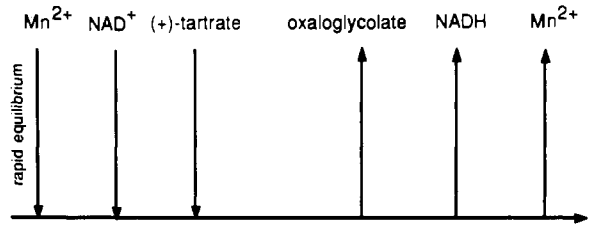

prior to binding of (+)-tartrate and NAD^+.

Table III summarizes the inhibition patterns and inhibition constants obtained for NADH, oxalacetate, and pyruvate. NADH is a competitive inhibitor versus NAD^+, and a noncompetitive inhibitor versus (+)-tartrate. Oxalacetate is a competitive inhibitor versus (+)-tartrate and an uncompetitive inhibitor versus NAD^+. These data indicate that NAD^+ adds to the enzyme prior to (+)-tartrate.

The kinetic mechanism for TDH-catalyzed oxidation of (+)-tartrate is shown in Scheme I. Mn^{2+} adds to free enzyme, followed by NAD^+ and (+)-tartrate. Oxaloglycolate is the first product released from the enzyme, followed by NADH and Mn^{2+}. The rate equation for this reaction is

$$v = \frac{V_{max}ABC}{K_{ia}K_{ib}K_c + K_{ia}K_bC + K_{ib}K_cA + K_bAC + K_cAB + ABC} \quad (8)$$

where A, B, and C represent the concentrations of Mn^{2+}, NAD^+, and (+)-tartrate, respectively. K_{ia} is the dissociation constant of A from EA, and K_{ib} is the dissociation constant of B from EAB. K_b and K_c are the Michaelis constants of B and C, respectively.

The initial velocity data obtained for the oxidation of D-malate (Table II) indicate that the kinetic mechanism is similar to that for (+)-tartrate oxidation. When the concentration of D-malate is varied at different free Mn^{2+} levels, the reciprocal plots intersect on the ordinate, indicating that Mn^{2+} adds to TDH in rapid equilibrium prior to D-malate addition. When D-malate concentration is varied at different levels of NAD^+, the reciprocal plots intersect to the left of the ordinate; thus, addition of NAD^+ and D-malate is sequential. NADH is a competitive inhibitor versus NAD^+, indicating that NAD^+ binds prior to D-malate. V_{max} for the oxidative decarboxylation of D-malate is 23.6 ± 0.2 μmol min^{-1} (mg of TDH)$^{-1}$; the Michaelis constants and Mn^{2+} dissociation constant are given in Table II.

To determine whether CO_2 or pyruvate is released first from the enzyme, they were tested as product inhibitors versus D-malate. Pyruvate is a noncompetitive inhibitor, which indicates that it can dissociate from the enzyme prior to CO_2 dissociation. Attempts to quantify CO_2 inhibition of D-malate oxidation were unsuccessful owing to the apparently low affinity of the enzyme for CO_2 (100 mM HCO_3^- was required to see any inhibition at all). Qualitatively, however, the inhibition appears to be noncompetitive, which suggests that pyruvate and CO_2 release is random. The kinetic mechanism for D-malate oxidation derived from the initial velocity studies is depicted in Scheme II.

pH Dependence of V and V/K. The pH profiles for the TDH-catalyzed oxidation of (+)-tartrate and D-malate are shown in Figure 1. For both reactions, the velocity decreases with decreasing pH; for (+)-tartrate oxidation, the variation of $(V/K)_{tartrate}$ with pH defines a pK of 6.51 ± 0.03, and the variation of V defines a pK of 6.63 ± 0.03. The V profile for D-malate oxidation reaches a limiting slope of 1 and shows a pK of 6.77 ± 0.06. The $(V/K)_{D\text{-malate}}$ profile defines a pK of 6.84 ± 0.10.[3]

Scheme II

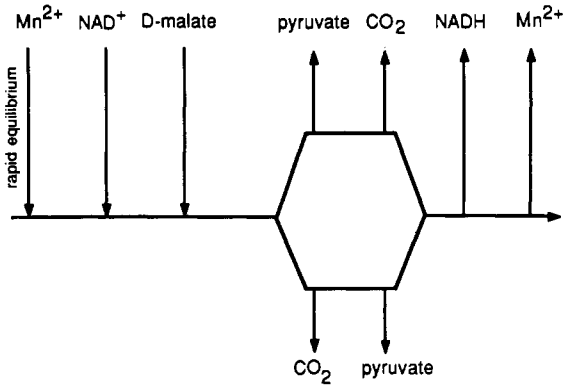

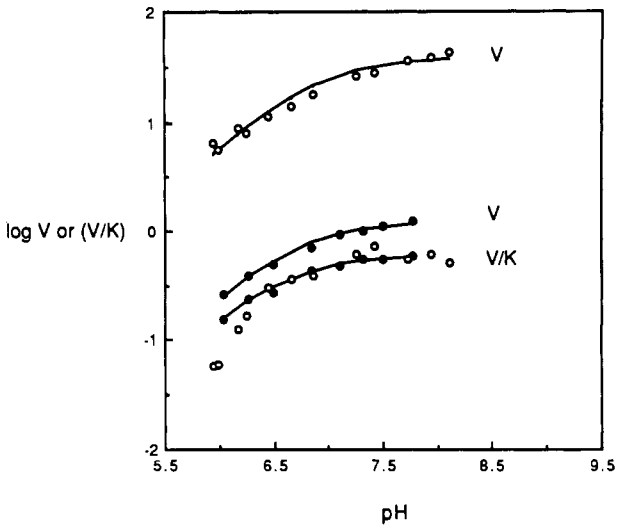

FIGURE 1: pH dependence of the kinetic parameters for tartrate dehydrogenase catalyzed oxidation of (+)-tartrate (●) and D-malate (○). (+)-Tartrate and D-malate were the varied substrates in these experiments. The solid lines represent the fit of the experimental data to eq 7. The fit to the $(V/K)_{D\text{-malate}}$ data has been omitted for clarity.

Determination of the Reaction Products. The ^1H NMR spectrum of the sample prepared by incubation of D-malate with tartrate dehydrogenase shows only a singlet at 2.38 ppm, identical with that observed for an authentic sample of pyruvate. The spectrum of the sample prepared by turnover of *meso*-tartrate consists of a doublet of doublets centered at 3.72 ppm (J = 6.0, 12.0 Hz), a doublet of doublets centered at 3.82 ppm (J = 3.0, 12.0 Hz), and a doublet of doublets centered at 4.09 ppm (J = 3.0, 6.0 Hz). This species was identified as glycerate by comparison with an authentic sample of D-glycerate. Finally, the product of the *meso*-tartrate reaction is a substrate for glyoxalate reductase using the coupled enzyme assay described by Ebbighausen and Giffhorn (1984), confirming that TDH produces D-glycerate from D-malate.

In order to determine whether the pyruvate that was identified by ^1H NMR as the product of D-malate oxidation arises from enzyme-catalyzed oxidative decarboxylation of D-malate or via nonenzymatic decarboxylation of enzyme-produced oxalacetate, the TDH-catalyzed oxidation of D-malate was carried out in the presence of lactate or malate dehydrogenase. Were tartrate dehydrogenase to produce and release oxal-

[3] Although the data in this experiment appear to be approaching a slope greater than unity, fitting the data to an equation describing ionization of two bases did not improve the fit significantly.

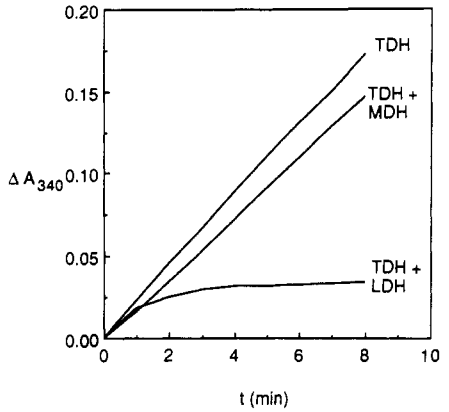

FIGURE 2: Trapping of the product of D-malate oxidation. The experiment was carried out in 100 mM HEPES, pH 8.0, containing 1.5 mM NAD^+, 0.5 mM D-malate, 0.4 mM $Mn(OAc)_2$, and 1 mM DTT. Each cuvette contained 0.001 unit of tartrate dehydrogenase and either 0 or 10 units of malate dehydrogenase or lactate dehydrogenase.

acetate, the presence of lactate dehydrogenase would not affect the rate of appearance of NADH, monitored at 340 nm; malate dehydrogenase, however, would trap the oxalacetate and reduce it to malate, recycling the NADH back to NAD^+. Therefore, in the presence of malate dehydrogenase, one would expect to see no increase in absorption at 340 nm over time. Conversely, were tartrate dehydrogenase to produce pyruvate directly from D-malate, the presence of malate dehydrogenase would not affect the appearance of NADH, and lactate dehydrogenase would prevent the accumulation of NADH by reducing pyruvate. As shown in Figure 2, malate dehydrogenase has little effect on the rate of appearance of NADH, while lactate dehydrogenase prevents the accumulation of NADH. Thus, it appears that tartrate dehydrogenase catalyzes the oxidative decarboxylation of D-malate.

Further evidence in support of this conclusion comes from the observation that TDH catalyzes the oxidation of NADH in the presence of pyruvate and CO_2, presumably via catalysis of the reverse reaction to produce D-malate.

Oxaloglycolate is suggested to be the product of (+)-tartrate oxidation because dihydroxyfumarate, the stable tautomer of oxaloglycolate, serves as a substrate for the reverse reaction. Furthermore, neither hydroxypyruvate nor oxalacetate, the expected products of oxidative decarboxylation of tartrate and of dehydration of tartrate, respectively, is detected in enzymatic coupled assays. The protons on oxaloglycolate undergo rapid exchange in D_2O and therefore are not observed in ^1H NMR spectra. Indeed, no ^1H signals are seen in ^1H NMR spectra of solutions of (+)-tartrate incubated with tartrate dehydrogenase.

Divalent Metal Ion Specificity. The divalent metal ion requirement for TDH-catalyzed oxidation of (+)-tartrate was investigated by using Mn^{2+}, Mg^{2+}, VO^{2+}, Co^{2+}, Ni^{2+}, and Zn^{2+}. Linear production of NADH over the course of several minutes was observed only with Mn^{2+} and Mg^{2+}. Very slow nonlinear time courses were observed with VO^{2+} and Zn^{2+}, while Ni^{2+} appeared to inactive the enzyme (or inhibit it in a time-dependent manner). It is not clear whether Co^{2+} is an effective activator of TDH because it is precipitated by DTT, which is necessary for TDH activity.

The dissociation constants of Mn^{2+} and Mg^{2+} in the (+)-tartrate and D-malate oxidation reactions are given Table II. For the oxidation of (+)-tartrate in the presence of Mg^{2+}, V_{max} is 0.296 ± 0.004 μmol min^{-1} mg^{-1}. For D-malate oxidation in the presence of Mg^{2+}, V_{max} is 12.0 ± 0.5 μmol min^{-1} mg^{-1}.

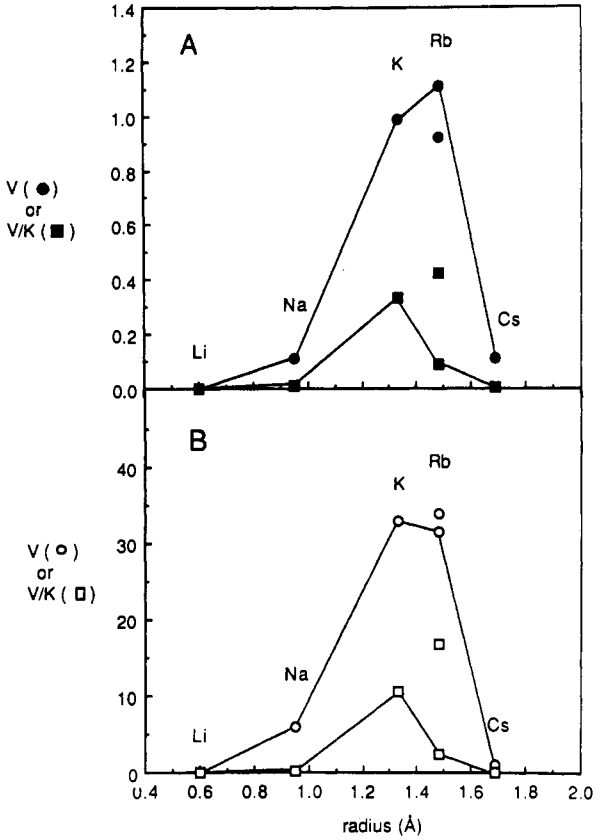

FIGURE 3: (A) V (●) and V/K (■) for (+)-tartrate oxidation catalyzed by tartrate dehydrogenase as a function of the monovalent cation. (B) V (○) and V/K (□) for D-malate oxidation catalyzed by tartrate dehydrogenase as a function of the monovalent cation. In both panels, the points not connected to the lines represent NH_4^+. Conditions are described under Materials and Methods.

Table IV: Michaelis Constants for Monovalent Cations in Tartrate Dehydrogenase Catalyzed Reactions

		K_m (mM)	
M^+	r (Å)	(+)-tartrate reaction	D-malate reaction
Li^+	0.60		
Na^+	0.95	13	52
K^+	1.33	2.9	3.1
Rb^+	1.48	12.5	14
NH_4^+	1.48	2.2	2.0
Cs^+	1.69	17	n.d.

Monovalent Cation Specificity. The alkali metals Li^+, Na^+, K^+, Rb^+, and Cs^+, as well as NH_4^+, were investigated as activators of TDH. The kinetic parameters for (+)-tartrate and D-malate oxidation are shown as a function of the ionic radius of the monovalent cation in Figure 3. The Michaelis constants for the monovalent cations in these reactions are given in Table IV.

DISCUSSION

Most enzymes exhibit stringent stereochemical requirements for binding and conversion of substrates to products. Thus, a number of microorganisms have separate pathways for the metabolism of each of the stereoisomers of tartrate (Clarke & Ornston, 1975). Kohn et al. (1968) reported isolation of a tartrate dehydrogenase from *P. putida* which oxidized (+)- and *meso*-tartrate to oxaloglycolate. We set out to investigate this enzyme in more detail and discovered that the (+)-tartrate oxidizing enzyme which we isolated from *P. putida* does indeed turn over both (+)- and *meso*-tartrate. However, only

Scheme III

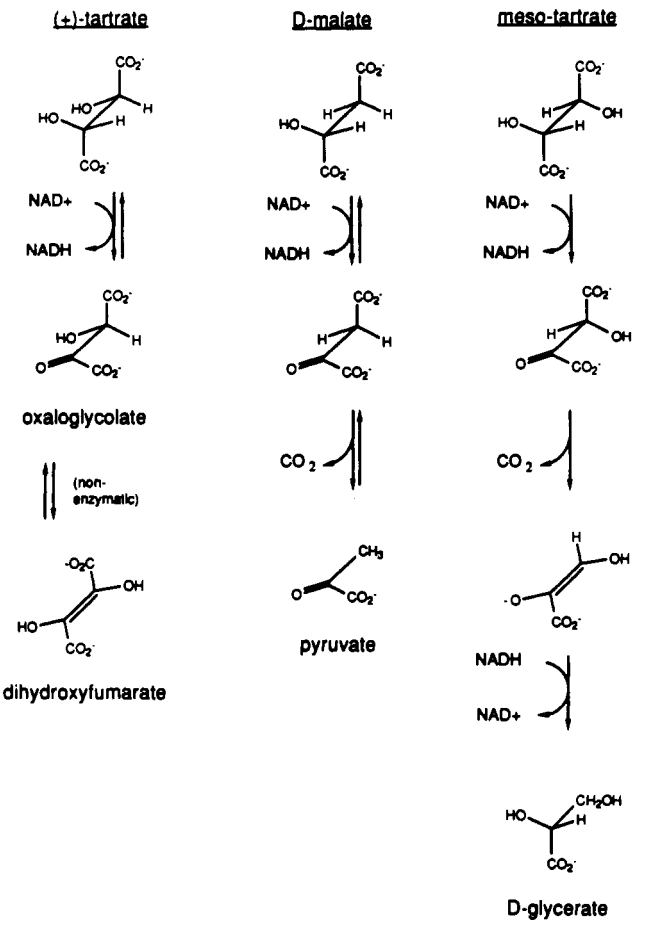

(+)-tartrate is converted to oxaloglycolate; *meso*-tartrate is decarboxylated to generate D-glycerate and CO_2. Furthermore, D-malate is an excellent substrate for the enzyme, undergoing oxidative decarboxylation to produce pyruvate and CO_2. Scheme III summarizes the reactions we observe, along with possible mechanisms.

The products arising from incubation of (+)-tartrate, *meso*-tartrate, and D-malate with TDH are identified by both ^{1}H NMR and enzymatic assays. Pyruvate is clearly identified in the ^{1}H NMR spectrum of the D-malate reaction. However, due to the instability of oxalacetate, especially in the presence of divalent metal ions, the NMR experiment does not distinguish between pyruvate formed as a result of enzyme-catalyzed oxidative decarboxylation of D-malate and pyruvate formed from decarboxylation of oxalacetate that was released into solution by the enzyme. Our failure to trap any oxalacetate in the presence of a high level of malate dehydrogenase, however, indicates that TDH catalyzes the oxidative decarboxylation of D-malate, forming pyruvate directly.

The ^{1}H NMR spectrum of the *meso*-tartrate reaction clearly shows that glycerate is the sole product. Ebbighausen and Giffhorn (1984) demonstrated that TDH from *R. sphaeroides* required catalytic amounts of NAD^+ for production of D-glycerate from *meso*-tartrate. Although we have not yet demonstrated the requirement for NAD^+ in this reaction with the *P. putida* enzyme, it is difficult to envision how the reaction might proceed without it. It seems reasonable to propose that D-glycerate is produced by transient NAD^+-dependent oxidation of *meso*-tartrate to form oxaloglycolate, which, rather than being released into solution, decarboxylates at the active site (Scheme III). The intermediate thus produced, which is the enolate of hydroxypyruvate, is then reduced by enzyme-bound NADH to yield D-glycerate, with no net production of NADH. Although the ^{1}H NMR spectrum does not identify the stereoisomer of glycerate that is formed, the fact that it is a substrate for glyoxalate reductase suggests that it is D-glycerate (Kohn & Warren, 1970). This is reasonable since (+)-tartrate and D-malate are oxidized at carbon centers with the *R* configuration and *meso*-tartrate would likely be oxidized at the carbon center with the same configuration; unless the oxidized intermediate rotates in the active site, return of the hydride would lead to production of D-glycerate.

The V/K vs pH profiles illustrated in Figure 1 indicate that catalysis of (+)-tartrate and D-malate oxidation requires that an ionizable group with a pK of about 6.7 be unprotonated. Because NAD^+, tartrate, and D-malate do not have a pK's in this region, the ionizable group is likely a residue on the enzyme. Consideration of a chemical mechanism for the catalytic reaction suggests that this residue functions as a base to remove the proton from the hydroxyl group at C2 during oxidation. Schimerlik and Cleland (1977), in their characterization of the pH dependence of the kinetic parameters for L-malate oxidation with pigeon liver malic enzyme, observed that catalysis required a group on the enzyme with a pK of 5.6–6 to be unprotonated. They ascribe to that group a role analogous to the one described above for the residue observed in TDH pH profiles. Interestingly, they also determined that catalysis required that a group with a pK of 8 be protonated; they suggested that the function of this acid catalyst is to protonate enolpyruvate formed upon decarboxylation of oxalacetate. Although the tartrate dehydrogenase catalyzed oxidative decarboxylation of D-malate is the same reaction as that catalyzed by malic enzyme, we do not see evidence for ionization of a group at high pH.

The pK's observed in the V_{max} profiles and V/K profiles are not significantly different from one another, which suggests that there are no pH-dependent steps following the first irreversible step in the catalytic cycle that are rate-limiting. Such steps, if they were present, would be manifested by a displacement of the pK seen in the V_{max} profile to lower pH relative to the pK seen in the V/K profiles (Cleland, 1982). Since (+)-tartrate and D-malate were the variable substrates in the experiments illustrated in Figure 1, and V/K represents conditions extrapolated to zero variable substrate concentration, the V/K profiles shown refer to the same enzyme form and are redundant. The fact that these two profiles overlay one another lends further support to the notion that a single protein is responsible for both catalytic activities.

A common function for divalent metal ions which do not undergo redox chemistry in enzymatic reactions is to stabilize enolate intermediates that arise in the course of the catalytic reaction (Jencks, 1969). Thus, for example, Zn^{2+} is presumed to stabilize the enolate intermediate in the aldol condensation of dihydroxyacetone phosphate with 3-phosphoglyceraldehyde catalyzed by yeast aldolase (Smith & Mildvan, 1981). Therefore, we were intrigued by the observation of Kohn et al. (1968) that tartrate dehydrogenase from *P. putida* catalyzed the Mn^{2+}- and K^+-dependent oxidation of (+)-tartrate to oxaloglycolate. There is no obvious chemical need for a divalent metal ion for the NAD^+-dependent oxidation of tartrate, and, although it remains possible that Mn^{2+} functions solely to facilitate binding, there are numerous enzymes which act on anionic substrates and yet do not require metal ions.

The finding that TDH catalyzes the decarboxylation of D-malate and *meso*-tartrate provides a rationale for the divalent metal requirement. It seems likely that the metal functions as an electron sink to facilitate the decarboxylation

of the β-keto acid formed as an enzyme-bound intermediate. The same role has long been postulated for the divalent metal ion in malic enzyme (Seltzer et al., 1959; Grissom & Cleland, 1988). The finding that oxidation of (+)-tartrate by TDH requires a divalent metal ion suggests that it may play a role in substrate binding as well.

It is interesting to note that the decreased catalytic activities of tartrate dehydrogenase in the presence of Mg^{2+} appear to arise largely from the weaker binding of Mg^{2+} relative to Mn^{2+}. Although the K_d for Mg^{2+} is approximately 40-fold higher than the K_d for Mn^{2+}, the maximal velocity attained in the presence of Mn^{2+} is only twice V_{max} in the presence of Mg^{2+}. These data suggest that Mg^{2+} and Mn^{2+} affect catalysis equally well, once they are in place in the active site. Grissom and Cleland (1988) have observed the same phenomenon in their study of chicken liver malic enzyme, which encompassed a wider range of divalent metal ions.

TDH also shows discrimination in the binding of monovalent cations. As shown in Table IV, the K_m's for different alkali metals vary approximately 20-fold, with the tightest binding being observed with K^+, and weaker binding occurring with larger and smaller alkali metals. More interesting, however, is the dependence of the apparent V_{max} on the ionic radius of the monovalent cation. Since the apparent V_{max} is independent of the affinity of the enzyme for the monovalent cation, the variation observed must be a reflection of the influence exerted by the monovalent cation on the binding of the other substrates, or perhaps on the conformation of the protein. The kinetic constants obtained for NH_4^+ appear anomalous with respect to the trends defined by the alkali metals, possibly because NH_4^+ can engage in hydrogen-bonding interactions that are not available to the alkali metals.

The conversion of *meso*-tartrate to D-glycerate, illustrated in Scheme III, shows that TDH has the potential to catalyze the sequential oxidation, decarboxylation, and reduction of its substrate. Each intermediate that is formed on this pathway could, in theory, either dissociate from the enzyme or react further. The various products that result from (+)-tartrate, D-malate, and *meso*-tartrate turnover appear to arise because each substrate yields an intermediate that dissociates from the enzyme at a different step of the catalytic pathway. Thus, the product of (+)-tartrate oxidation dissociates upon formation, but the products of D-malate and *meso*-tartrate oxidation remain bound and undergo decarboxylation. Pyruvate dissociates, but hydroxypyruvate, or its enol tautomer, does not, and is reduced to glycerate by NADH. The product that results from a given substrate is therefore determined by the relative energy barriers for dissociation and for further reaction for each intermediate.

ACKNOWLEDGMENTS

Kinetic studies were carried out in the laboratory of Dr. John Blanchard, who also provided stimulating discussion throughout the course of this work.

REFERENCES

Bradford, M. M. (1976) *Anal. Biochem. 72*, 248.

Clarke, P. H., & Ornston, L. N. (1975) in *Genetics and Biochemistry of Pseudomonas* (Clarke, P. H., & Richmond, M. H., Eds.) pp 271–275, John Wiley and Sons, London.

Cleland, W. W. (1979) *Methods Enzymol. 63*, 103–138.

Cleland, W. W. (1982) *Methods Enzymol. 82*, 390–405.

Duclaux, E. (1920) *Pasteur; the History of a Mind*, pp 43–46, W. B. Saunders Company, Philadelphia.

Ebbighausen, H., & Giffhorn, F. (1984) *Arch. Microbiol. 138*, 338–344.

Grissom, C. B., & Cleland, W. W. (1988) *Biochemistry 27*, 2927–2934.

Jencks, W. P. (1969) *Catalysis in Chemistry and Enzymology*, pp 119–120, Dover Publications, Inc., New York.

Kohn, L. D., & Warren, W. A. (1970) *J. Biol. Chem. 245*, 3831–3839.

Kohn, L. D., Packman, P. M., Allen, R. H., & Jakoby, W. B. (1968) *J. Biol. Chem. 243*, 2479–2485.

Martell, A. E., & Smith, R. M. (1977) *Critical Stability Constants*, Vol. 3, Plenum Press, New York.

Schimerlik, M. I., & Cleland, W. W. (1977) *Biochemistry 16*, 576–583.

Seltzer, S., Hamilton, G. A., & Westheimer, F. H. (1959) *J. Am. Chem. Soc. 81*, 4018–4024.

Shilo, M., & Stanier, R. Y. (1957) *J. Gen. Microbiol. 16*, 482–490.

Smith, G. M., & Mildvan, A. S. (1981) *Biochemistry 20*, 4340–4346.